A Green Amino Acid-based Solvent Blended with Diethanolamine Solution for CO2 Capture Using Micro-contactor

Forough Karimi
  Kermanshah University of Technology

Peyvand Valeh-e-Sheyda (✉ p.valeh-sheyda@kut.ac.ir)
  Kermanshah University of Technology   https://orcid.org/0000-0002-8270-3118

Research Article

A Green Amino Acid-based Solvent Blended with Diethanolamine Solution

for CO$_2$ Capture Using Micro-contactor

Forough Karimi[a], Peyvand Valeh-e-Sheyda[a,1]

[a] Chemical Engineering Department, Kermanshah University of Technology, Kermanshah, Iran.

Abstract

The core for carbon dioxide capture is the development of green solvents for absorption processes. The current research aims at the CO$_2$ capture process from a gas stream in a micro-contactor using an amino acid-based green technology containing diethanolamine (DEA) and L-arginine (ARG) solutions. The gas-liquid mass transfer performance has been experimentally assessed in terms of CO$_2$ absorption efficiency (%) and volumetric gas-phase mass transfer coefficient (K_Ga_V). The measurements have been carried out under liquid flow rate (Q_L: 3.0-9.0 ml/min), gas flow rate (Q_G: 120.0-300.0 ml/min) at a constant temperature of 45 °C, and atmospheric pressure. The aqueous composition of the blended solution was DEA ARG (35 0 wt%), DEA ARG (31 4 wt%), DEA ARG (27 8 wt%), and DEA ARG (23 12 wt%). It was found that an increase in the solvent flow rate from 3.0 to 9.0 ml/min enhanced the absorption efficiency, K_Ga_V, and N_Ga_V by 2.5%, 12.8%, and 2.6%, respectively. However, an increase in the gas flow rate from 120.0 to 300.0 ml/min reduced the efficiency by 6% but improved the K_Ga_V and N_Ga_V by 88% and 225%, respectively. Additionally, the K_Ga_V values followed a declining trend as the contribution of the DEA in the blended solution increased. Based on RSM modeling, the correlations for predicting the K_Ga_V and CO$_2$ absorption efficiency into blended DEA-Arg were successfully established

---

[1] Corresponding author. Tel.: +98 8338305000; fax: +98 8338305006. E-mail address: p.valeh-sheyda@kut.ac.ir

versus independent process variables. According to the optimization results, the maximum absorption efficiency and K_{Gav} were attained at 92.93% and 69.40 kmol/m^3.h.kPa for Q_L of 9.0 ml/min, Q_G of 263.4 ml/min, $C_{DEA-ARG}$ of (23 12 wt%). Comparing the gas-liquid mass transfer characteristics of the blended DEA-ARG with conventional secondary amine, DEA, in the T-shaped micro-contactor illustrated that presence of L-arginine amino acid with high concentrations of 12 wt%, as a promoter for CO_2 capture, can boost the performance of CO_2 absorption process.

Keywords: DEA-ARG blend, Micro-contactor, CO_2 absorption, Mass transfer coefficient, Response surface methodology.

1. Introduction

In recent years, human activities lead to the emissions of greenhouse gases such as CO_2, NO_2, and CH_4, causing global temperatures to rise (Dang et al. 2020). Of all greenhouse gases, carbon dioxide accounts for 65% of the gas emissions, which is dominantly emitted by burning fossil fuels. Thus, diverse cost-effective technologies considered to capture CO_2 from the gas phase (Chuah et al. 2019). These technologies utilized in the laboratory and on an industrial scale are mainly based on two theoretical approaches namely physical and chemical absorption processes (Chowdhury et al. 2020, Ghaemi &Behroozi 2020, Sreedhar et al. 2020), membrane separation (Nadeali et al. 2020), and molecular sieve adsorption (Lei et al. 2020, Yang et al. 2020).

Among all these methods, the solvent absorption process is a highly-efficient established technology that is commercially used for capturing CO_2 in the natural gas treatment industry (Dutcher et al. 2015). However, screening the solvents with appropriate absorption capacity is identified as the most important criterion affecting the CO_2 capture cost in the chemical absorption

2

45 procedures. The promising candidate is selected based on the absorption rate, the energy required

46 for reduction, degradation rate, solvent viscosity, solvent corrosion, volatility, price, precipitation,

47 boiling point, and vapor pressure. In this regard, amine solutions have been widely employed as

48 the most economical solvents in gas sweeteninlg and CO_2 capture units even at low pressures

49 because of their reasonable price, high chemical activity, and ability to reduce carbon dioxide up

50 to ppm (Morken et al. 2019). The commonly used amine-based solvents are monoethanolamine

51 (MEA) (Wang et al. 2019), 2-amino-2-methyl propanol (AMP) (Nwaoha et al. 2018), methyl

52 diethanolamine (MDEA) (Hosseini-Ardali et al. 2020), diglycolamine (DGA) (Zahid et al. 2017),

53 and piperazine (PZ) (Du et al. 2017, Fashi et al. 2020), etc.

54 MEA was the most widely used solvent in gas treating processes due to its tendency to react with

55 CO_2, low solvent cost, and high CO_2 capacity. Nevertheless, due to the high energy requirement

56 for regeneration, solvent loss, and oxidative degradation, the possibilities of employing other

57 solvents have to be examined for low-pressure operations (Rochelle 2012). Secondary amines like

58 Diethanolamine (DEA) are much less reactive, but their reaction products are not particularly

59 corrosive. They have high thermal stability and low energy consumption (Muchan et al. 2017).

60 These all make the aqueous solution of DEA to be an appealing alternative for post-combustion

61 CO_2 absorption. Unfortunately, the drawback of DEA is that it shows slow kinetics. As a result, a

62 suitable alternative additive is required to primarily promote its reaction rate and secondly enhance

63 the absorption capacity of the amine-based solvent in acid gas treating processes (Hasib-ur-

64 Rahman et al. 2012, Pashaei et al. 2021).

65 Amino acids have been examined to attain a potential substitute promoter for their oxidative

66 stability and sight volatility. Amino acids consist of carboxylic acid, amine groups, and a particular

67 side chain, having a strong basic character, which strongly determines their chemical and physical

68 features (Afkhamipour &Mofarahi 2018). At present, $_L$-arginine has gained extensive concern as

69 a promising co-promoter for CO_2 capture. Upon biological source of the $_L$-arginine, the amino acid

70 possesses the biodegradation characteristics, making it inherently reliable for the environment

71 (Kortunov et al. 2015).

72 The chemical CO_2 capture relies strongly on the interfacial mass transfer. Recently, microfluidic

73 techniques have been successfully applied to intensify the CO_2 mass transfer performance of two

74 gas-liquid contacting phases due to their safety, high surface-to-volume ratio, short transmission

75 distances, and controllability (Lam et al. 2013). The driving force gradient, reaction rates, and

76 mass transfer efficiency obtained by micro-contactors have presented great advantages over the

77 conventional technologies. Furthermore, to limit the high operating cost of the large reactors and

78 conform to the production capacity of the micro-reactors, the scaling out principle is utilized rather

79 than scaling up (Yu 2016).

80 Until now, the gas-liquid mass transfer and the flow pattern in micro-reactors have been

81 extensively inspected, and numerous models have predicted the mass transfer coefficients.

82 Kittiampon et al. (Kittiampon et al. 2017) investigated the CO_2 capture process in a T-type micro-

83 contactor using an aqueous ammonia solution to evaluate the interaction influences of temperature,

84 pressure, liquid flow rate, and solvent concentration. The maximum CO_2 absorption removal of

85 96.45% was obtained under temperature absorption of 30 °C, gauge pressure 300 kPa, 10 wt%

86 ammonia concentration, and liquid flow rate of 0.0003 m^3/hr. The experimental mass transfer

87 characteristics of the CO_2 absorption in an aqueous ionic liquid solution of 1-butyl-3-

88 methylimidazolium tetrafluoroborate, [bmim][BF4], illustrated that the liquid side volumetric

89 mass transfer coefficient would be significantly strengthened by increasing the gas to liquid flow

90 rate ratio and the ionic liquid concentration in the square cross-section microchannel. Meanwhile,

91 the length of the mass transfer zone would decline due to the reduction in the bubble velocity (Chu

92 et al. 2019). The findings of the CO_2 absorption capacity in a microchannel contactor demonstrated

93 that adding 2.2 M of monoethanolamine into water (1:1 molar ratio of MEA-to-CO_2) may

94 dramatically boost the absorption efficiency from 56.2% to 80.2% (Akkarawatkhoosith et al.

95 2020). Ganapathy et al. (Ganapathy et al. 2016) inspected the mass transfer and hydrodynamics

96 behavior of liquid-gas CO_2 capture into an aqueous DEA solution using a micro-structured reactor.

97 Under the slug and slug annular flow rates (Re_G: 15-151; Re_L: 19-93), the presented micro-

98 structured reactor provided the mass transfer coefficients as high as 17 s^{-1}, which was 1-3 orders

99 of magnitude higher as compared to conventional absorption contactors. Zhu et al. (Zhu et al.

100 2020) systematically monitored the gas-liquid distribution and mass transfer of CO_2 capture

101 process into sodium glycinate aqueous solution in a novel micro-reactor containing parallel multi-

102 channels. Employing a high-speed camera, they found slightly lower values of the average liquid

103 side volumetric mass transfer coefficient than a single channel, illustrating the excellent

104 distribution and mass transfer characteristics of the applied multi-channel micro-reactor.

105 The summary of the above microchannel literature review reveals that comprehensive mass

106 transfer studies have focused on the absorption of acid gas concerning the feed gas and solvent

107 concentrations, hydraulic diameter, length of mass transfer zone, solvent concentration, and

108 pressure drop, which are significant for the operating design and utilization of the micro-

109 contactors. In comparison, fewer CO_2 absorption works have paid attention to the capability of the

110 amino acids in the aqueous amine solutions for industrial CO_2 treatment processes. Thus,

111 additional experimental studies are still required to evaluate the effectiveness of the green solvent

112 technology as an alternative to the traditional aqueous solution of alkanolamine. In the current

113 study, L-arginine amino acid was selected as a promoter in aqueous 35% DEA to capture carbon
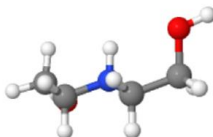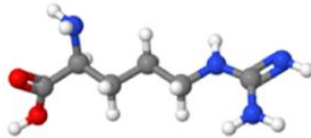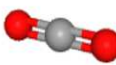
5

114 dioxide in a T-type micro-contactor. The contribution of the prompter concentration, the gas, and

115 liquid phase flow rate is varied to potentially assess the combination mass transfer performance of

116 the blended DEA-ARG solution in terms of the overall gas-phase mass transfer coefficient and

117 CO_2 absorption efficiency under the constant temperature and pressure.

118

119 **2. Experimental Section**

120 2.1. Chemicals

121 A secondary alkanolamine, diethanolamine (DEA, $C_4H_{11}NO_2$, industrial grade), carbon dioxide

122 (CO_2, >99.9, Alborz Persian Gas), and Arginine (ARG, $C_6H_{14}N_4O_2$, 99.0 Merck KGaA) were used

123 as received without further treatment. The provenance, purity, and molecular structure of the

124 chemicals utilized in CO_2 capture experiments are displayed in Table 1.

125

126 Table 1. The provenance, purity, and molecular structure of the materials used in the

127 experiments.

Material name	Solubility	Purity (%)	Supplier	Purification method	Structure
Diethanolamine (DEA)	Miscible in water	Industrial grade	Ilam gas company	None	
L-arginine (ARG)	14.87 g/100 ml water (20°C)	≥99.0	Merck KGaA	None	
Carbon dioxide (CO_2)	1.45 g/l water (25°C)	>99.9	Alborz Persian Gas	None	

128

129 2.2. Experimental equipment

6

130   Fig. 1 depicts the schematic view of the experimental apparatus employed for measuring the mass

131   transfer characteristics of CO_2 in the secondary amine and amino acid solutions. As seen, it consists

132   of a micro-contactor with internal diameter ID= 800 µm, and length L= 295 mm, a water bath, a

133   heater, a thermocouple thermometer (model ST-612), two mass flow controllers (GPC series-

134   BREEZENS, Apasco, Iran), a CO_2 gas sensor (Cozir CM-0123, Germany), a peristaltic pump

135   (BT01-YZ1515, China). To inspect online and save the changes in the CO_2 concentrations, the

136   CO_2 sensor was attached to a monitoring unit and a PC.
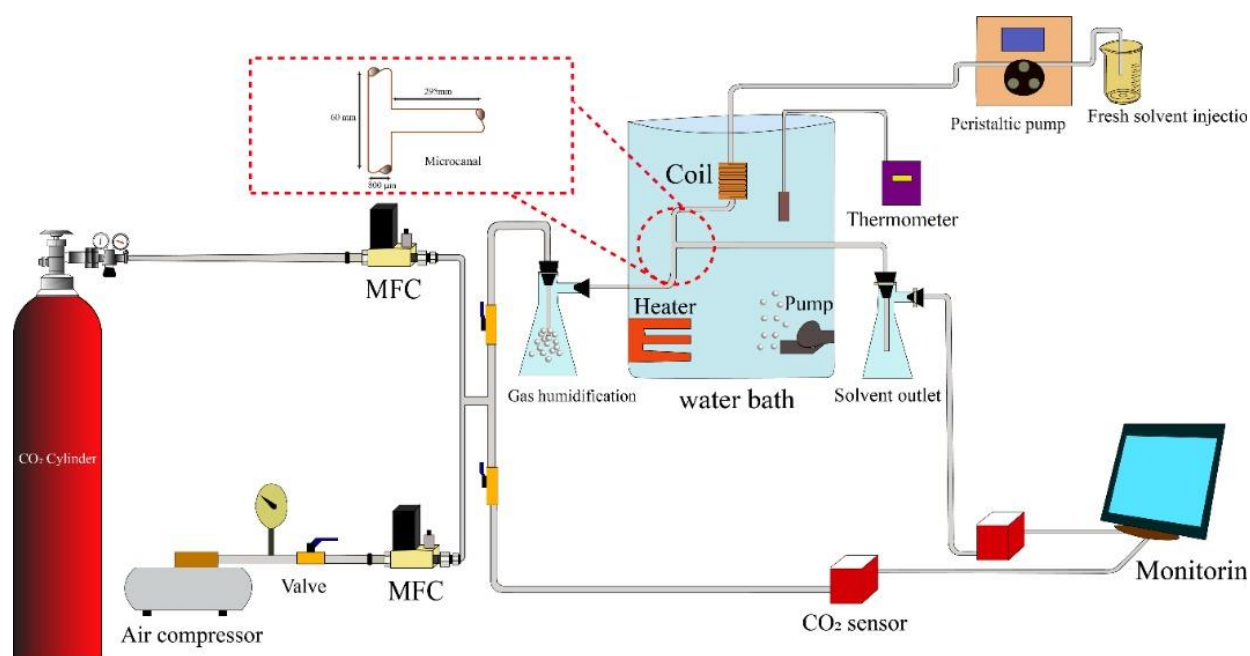

Fig. 1. Experimental setup used to assess CO_2 capture performance in the promoted DEA
solution with amino acid.

137

138   2.2. Experimental procedure

139   The CO_2 capture experiments in the prompted DEA solutions were measured at the fixed 35 wt%

140   of diethanolamine-amino acid under isothermal conditions of 45 °C. Before the experiments, four

141   aqueous systems of the mixed DEA: ARG with the mass ratio of 35:0, 31:4, 27:8, and 23:12 were

142   prepared. The micro-contactor was then placed in a water bath with the designed absorption

7

143 temperature of 45 °C, monitored via a thermometer with ±0.1 °C precision. The needed 15 vol%

144 CO_2 was obtained in CO_2 absorption experiments by employing two MFCs to regulate the flow

145 rates of CO_2 and compressed air. The total gas flow rate was then fixed in the designed range and

146 passed through a gas humidification chamber to be moisturized. The gas mixture was then

147 introduced into the micro-contactor section. Simultaneously, the aqueous blended absorbent with

148 given concentrations and volumetric flow rate of 3.0-9.0 ml/min was pumped from the vessel into

149 the micro-contactor using the peristaltic pump. Upon impinging the gas and liquid streams in the

150 micro-contactor, the CO_2 absorption process was carried out; the gas-liquid mixture flowed

151 downward into a phase separator through a connection tube. The CO_2 concentration at the inlet

152 and outlet gas streams was then analyzed employing the CO_2 analyzer. All experimental runs were

153 repeated three times, and the averaged data was given in the results.
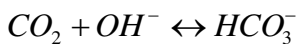
154

155 **3. Theoretical Aspect**

156 3.1. Reaction mechanism of CO_2 into promoted DEA solution

157 Danckwerts (Danckwerts 1979) reestablished the mechanism introduced originally by Caplow

158 (Caplow 1968) to depict the reaction between aqueous secondary alkanolamine and CO_2 (Eqs. 1-

159 3). The reaction primarily takes place in the liquid phase of the CO_2-DEA+arginine+H_2O interface

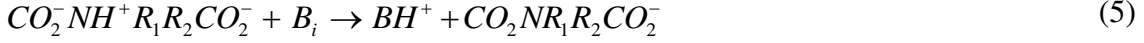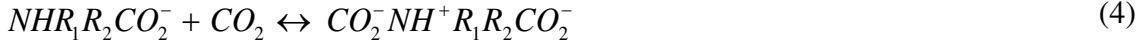160 via the formation of zwitterion, followed by the deprotonation in the basic media, B, as follows:

Carbamate formation: (1)

$$CO_2 + 2R_1R_2NH \leftrightarrow R_1R_2NCOO^- + R_1R_2NH_2^+$$

Bicarbonate formation: (2)

$$CO_2 + OH^- \leftrightarrow HCO_3^-$$

Carbonic acid formation: (3)

$$CO_2 + H_2O \leftrightarrow HCO_3^- + H^+$$

$$NHR_1R_2CO_2^- + CO_2 \leftrightarrow CO_2^-NH^+R_1R_2CO_2^- \tag{4}$$

$$CO_2^-NH^+R_1R_2CO_2^- + B_i \rightarrow BH^+ + CO_2NR_1R_2CO_2^- \tag{5}$$

161   Finally, according to successive reactions of 2 and 3, L-arginine amino acid ($NHR_1R_2CO_2^-$) forms

162   the intermediate complex ($CO_2^-NH^+R_1R_2CO_2^-$), and carbamate ($CO_2^-NR_1R_2CO_2^-$) is formed from

163   the proton removal by any base (B_i) (Mahmud et al. 2019).

164

165   3.2. Absorption efficiency and overall mass transfer coefficient

166   The efficiency of the CO_2 absorption, θ, is defined based on the following equation:

$$\theta(\%) = \left(1 - \left(\frac{y^{out}}{1 - y^{out}}\right)\left(\frac{1 - y^{in}}{y^{in}}\right)\right) \times 100 \tag{6}$$

167   Where y^{in} and y^{out} are the number of CO_2 moles at the inlet and outlet of the micro-contactor.

168   Considering the broad applications of amines in gas-liquid contactors, calculating and optimizing

169   the volumetric mass transfer coefficient based on the gas phase, K_Ga_V, is essential in determining

170   the absorption column height. The K_Ga_v parameter is experimentally measured based on the CO_2

171   concentration in the gas phase along with the gas-liquid contactor (Afkhamipour &Mofarahi

172   2018). The overall volumetric mass transfer coefficient based on the gas phase, K_Ga_V, can be

173   computed at the interface as follows:

$$K_Ga_V = \frac{G}{ZP}\left[\ln\left(\frac{Y_{in}}{Y_{out}}\right) + \left(Y_{in} - Y_{out}\right)\right] \tag{7}$$

174   where Y_{in} and Y_{out} represent the molar ratio of CO_2 at the micro-contactor inlet and outlet. The

175   parameters of P (kPa), Z (m), and G (kmol/h.m^2) denote the total pressure, micro-contactor length,

176   and input gas flow rate, respectively.

177   The volumetric molar flux expresses the rate of CO_2 transferred per volume unit of the absorbed

178   region from the gas to the liquid phase and is given from the following equation.

$$N_a a_V = \frac{G}{Z}\left(Y_{in} - Y_{out}\right) \tag{8}$$

179

180   3.3. Response surface methodology (RSM)

181   Response Surface Methodology (RSM), based on the full factorial design (FFD) approach (Tarley

182   et al. 2009), is employed to scrutinize the efficiency of CO_2 capture characteristics, namely θ,

183   K_{Ga_v}, and $N_{A}a_V$, versus the amino acid concentration, the gas and liquid flow rates. Table 2 reports

184   the operating range of each variable in the FFD experimental design.

185   Table 2. The levels of independent variables for CO_2 capture process (DEA wt%=35-C_{ARG}).

Symbol	Input variable	Units	Minimum	Maximum	Mean
A	Q_L	ml/min	3.0	9.0	6.0
B	Q_G	ml/min	120.0	300.0	210.0
C	$C_{ARG-DEA}$	wt%	4-31	12-23	8-27

186   The FFD procedure recommended a quadratic prediction model to design the experimental runs,

187   as given below (Khuri &Mukhopadhyay 2010):

$$y = \beta_0 + \sum_{i=1} \beta_i X_i + \sum_{i=1} \beta_{ii} X_i^2 + \varepsilon \tag{9}$$

188   where y is the response function, β_0 denotes the constant parameter, β_i, β_{ii}, X_i, and X_j demonstrate

189   the coefficients of linear expression, quadratic term, and the coded quantities of factors i and j,

190   respectively. The term ε is the unanticipated expression calculated experimentally. Eq. (9) can fit

191   the empirical data by utilizing the least-squares method and multiple regression analysis. This

192   method generates the β term by minimizing the residual value. The proposed model describes the

193   performance of the corresponding response in the experimental range as an independent variable.

194   Finally, the analysis of variance (ANOVA), as a beneficial statistical procedure for the model

195   quality, was explored to assess the statistical variables, proportionality adequacy, and the efficacy

196   of the developed model by examining the principles of empirical variance (Behroozi et al. 2021).

197

198   **4. Results and discussion**

199   4.1. Effect of amino acid concentration

200   Fig. 2 outlines the experimental results of the carbon dioxide absorption efficiency, Θ (%), and the

201   volumetric gas-phase mass transfer coefficient, K_Ga_V (kmol/m^3.h.kPa), versus different

202   concentrations of ARG-DEA. It is of note that the total concentration of the blended solvent was

203   chosen 35 %wt for the single DEA aqueous solution and the portions of the DEA by the ARG

204   amino acid. As such, to assess the effect of the attendance of the amino acid in the aqueous

205   alkanolamine solution, the values of the CO_2 absorption efficiency and the volumetric gas-phase

206   mass transfer coefficient are compared in single aqueous solution of DEA and the total blended
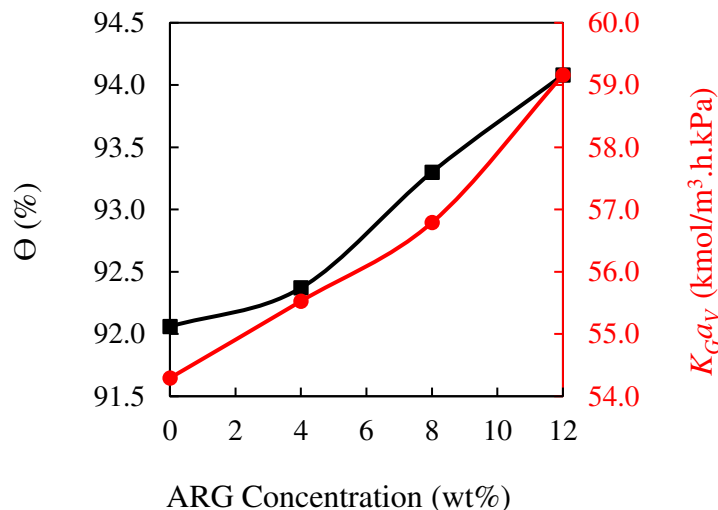
207   solution of 35 % DEA-ARG.

Fig. 2. CO_2 absorption efficiency and volumetric gas-phase mass transfer coefficient versus ARG concentration on under 35 %wt DEA, Q_G= 210.0 ml/min and Q_L= 6.0 ml/min.

208

209   Compared to the results for the aqueous DEA solvent (35 % wt), it is observed that at a given flow

210   rate of gas and solvent streams, high concentrations of ARG to 12 %wt in the total blend of ARG-

211   DEA aqueous solution intensifies the CO_2 capture from 92.06% to 94.08%. Under the same

212   operating condition inside the micro-contactor, the rise in the amino acid concentration enhances

213   the $K_G a_V$ values by 8.96%. This is in line with the findings of the previous works illustrating that

214   adding ARG enhances the CO_2 equilibrium solubility in a total aqueous 40 % (DEA-ARG) system

215   at a fixed temperature (Haghtalab &Gholami 2019). The presence of the guanidinium group in the

216   arginine side chain allows the fast deprotonation from the CO_2-amino acid complex, enabling the

217   carbamate formation, thus, exhibiting superior CO_2 absorption capacity (Zhang et al. 2012).

218   Furthermore, all the amine-amino acid systems are basic and the increase in the presence of amino

219   acid in DEA solution intensifies the pH values of the blended DEA-ARG mixtures, resulting in

220   the enhancement of CO_2 solubility in these systems.

221

222   4.2. Effect of inlet liquid flow rate

223   As indicated in Fig. 3, under the high concentrations of the ARG, the values of carbon dioxide

224   absorption efficiency and the overall gas phase mass transfer coefficients follow a rising trend with

225   increasing the promoted liquid flow rate. An increase in liquid flow rate 3.0 to 9.0 ml/min yielded

226   an increment of 2.5% and 12.8% in the values of the Θ (%) and $K_{G}a_V$. Specifically, at a constant

227   gas flow rate of 210 ml/min and absorption temperature of 40 °C, the maximum value of the $K_{G}a_V$

228   =60.53 kmol/m^3.h.kPa was found for the sample with a liquid flow rate of 9.0 mL/min.
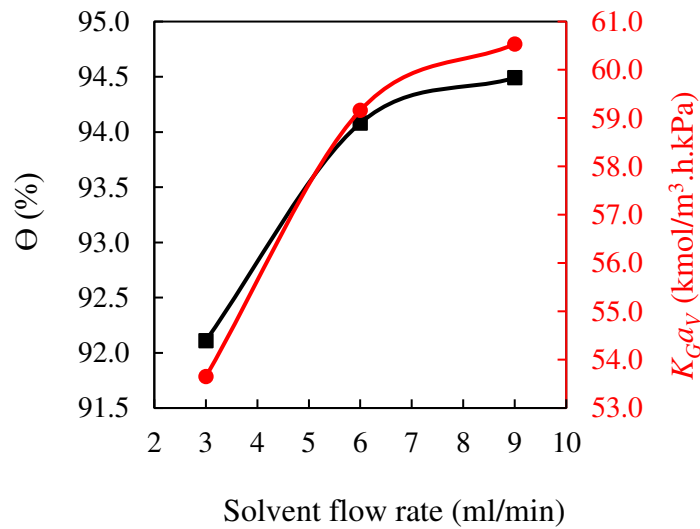

Fig. 3. CO$_2$ absorption efficiency and gas-phase mass transfer coefficient versus the inlet
liquid flow rate on at C$_{DEA-ARG}$ (23 12 wt%), T=45 °C, and Q_G =210.0 ml/min

229

230   In the sense of CO$_2$ absorption efficiency, the growth in the solvent flow rates keeps the arginine

231   content inside the micro-contactor higher, resulting in the augmentation in the driving force for

232   obtained Θ values (Constantinou &Gavriilidis 2010). In the sense of $K_{G}a_V$, increasing the solvent

233   flow rate strengthens the effective interfacial area of the gas-liquid so that the liquid film

234   surrounding the bubbles will be extended. Correspondingly, a thicker liquid film will be formed,

235   which could prevent the fluid film saturation in the micro-contactor and the gas-liquid mass

13

236 transfer (Niu et al. 2009). However, based on the results in Fig. 3, further increase in the inlet

237 solvent flow rate will not intensify the absorption rate since the upward slope of Θ and $K_{G}a_V$ are

238 reduced, which in turn will lead to the solvent loss (Su et al. 2010). The results are also in

239 accordance with that in the literature (Rashidi et al. 2022).

240 For the sake of solvent formulation, it is essential to assess the CO_2 absorption performance of

241 blended amine- amino acid with that of single secondary alkanolamines, particularly DEA .The

242 relative mass transfer flux, $N_{DEA+ARG}a_V / N_{DEA}a_V$, versus the inlet solvent flow rate in Fig. 4

243 illustrates the contribution of arginine at high concentrations of 12 %wt enhancing the volumetric
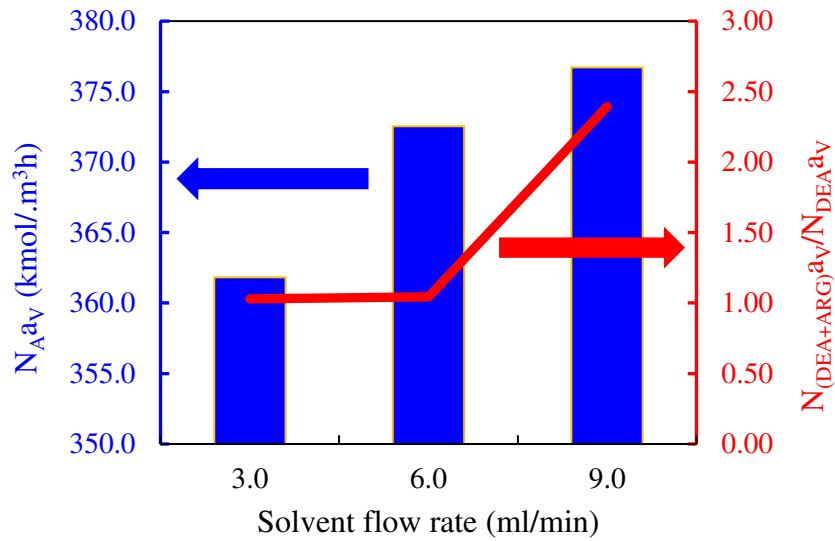
244 mass flux in the designed micro-contactor.

Fig. 4. The mass transfer flux and the relative mass transfer flux versus the inlet liquid flow rate at T=45 °C, Q_G = 300.0 ml/min, and $C_{DEA-ARG}$ (23 12 wt%).

245

246 According to the figure, in the blended aqueous DEA-ARG solution and for a constant feed gas

247 flow rate of 300 mL/min, the maximum CO_2 mass transfer flux of about 376.70 kmol/m^3.h can be

248 attained at the inlet solvent flow rate of 9 mL/min. Besides, the increment slope in the values of

249 the relative volumetric mass transfer flux demonstrates that the intensification in the volumetric

250 molar transfer flux with high concentrations of ARG is superior at high liquid flow rates in the

251 aqueous DEA-ARG solutions.

252

253 4.3. Effect of feed gas flow rate

254 Fig. 5 reveals the results of the CO_2 absorption efficiency and volumetric gas-phase mass transfer

255 coefficient versus different ranges of the feed gas flow rate under the absorption temperature of 45

256 °C and inlet solvent flow rate of 6 ml/min. As depicted in Fig. 6, at low feed gas flow rates of 120

257 ml/min, the CO_2 absorption is higher than 95%. At a constant liquid flow rate of 6.0 ml/min, upon

258 elevating the gas flow rate from 120.0 to 300.0 ml/min, the absorption efficiency was found to fall

259 in the range of 95.7- 90.0 %. The reduction is due to the increase in the gas velocity, thereupon,

260 the decrease in the gas-liquid contact time. Consequently, the CO_2 concentration will increase at

261 the micro-contactor outlet, and thus, the absorption level declines. In the given solvent flow rate,

262 the rise of the inlet gas flow rate brings about a substantial enhancement in the volumetric gas-

263 phase mass transfer coefficient. As seen, for the blended aqueous solution of DEA ARG (23 12

264 wt%), the value of K_{GaV} will raise from 37.40 kmol.m^3.h.kPa at Q_G of 120 ml/min to 62.98

265 kmol.m^3.h.kPa at Q_G of 300 ml/min. The augmentation in the mass transfer by rising the gas flow

266 rate results from the flow circulation in the solvent slugs, and surface renewal of the liquid film

267 originated from expanding the superficial gas velocity in the designed micro-contactor. This is

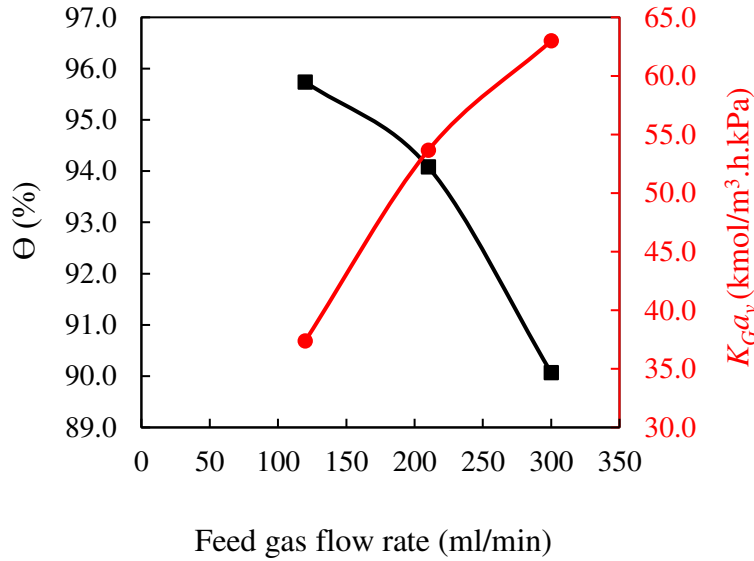268 explained in the literature frequently (Afkhamipour &Mofarahi 2017).

269

15

Fig. 5. CO_2 absorption efficiency and volumetric gas-phase mass transfer coefficient versus gas flow rate on at T=45 °C, Q_L =6.0 ml/min, C $_{DEA-ARG}$ (23 12 wt%).

270 Based on the variations of volumetric gas-phase mass transfer coefficients with gas and liquid flow

271 ratios, the dominant resistance is the mass transfer resistance in the liquid film since the rise in the

272 liquid-phase flow rate did not change the K_Ga_V as the gas flow did. Thus, the increment of Q_L can

273 reduce the mass flow resistance, leading to higher CO_2 absorption efficiency. However, it has an

274 optimum point that surpasses the quantity with the lowest economic design, thus increasing solvent

275 consumption and recovery cost. Furthermore, as the absorption process is conducted in the micro-

276 contactor, the mass transfer coefficient and interfacial area are greater than those in the standard

277 mass transfer systems due to fluid properties flowing through the micro-contactor as reported in

278 the literature (Afkhamipour &Mofarahi 2018). Thus, the mass transfer coefficient using micro-

279 contactors is higher than via other devices, making a high-efficient CO_2 absorption process.

280 The trend of mass transfer flux and relative mass transfer flux with gas flow rate has been

281 illustrated in Fig. 6. It is observed that under the given solvent flow rate, rising the inlet gas flow

282 rate linearly enhances the volumetric molar transfer flux of the blended solvent from 157.04 to

16

283   372.53 kmol/h.m^3, which is in line with the observed overall gas-phase mass transfer coefficient.

284   Besides, the experimental values of the relative molar transfer flux, $N_{DEA+ARG}a_V/N_{DEA}a_V$, illustrate

285   that by adding arginine in the new blends, DEA ARG (23 12 wt%), the CO_2 absorption intensifies

286   by 1.045. Accordingly, the suggested mixture of DEA-ARG solvent could decline CO_2 capture

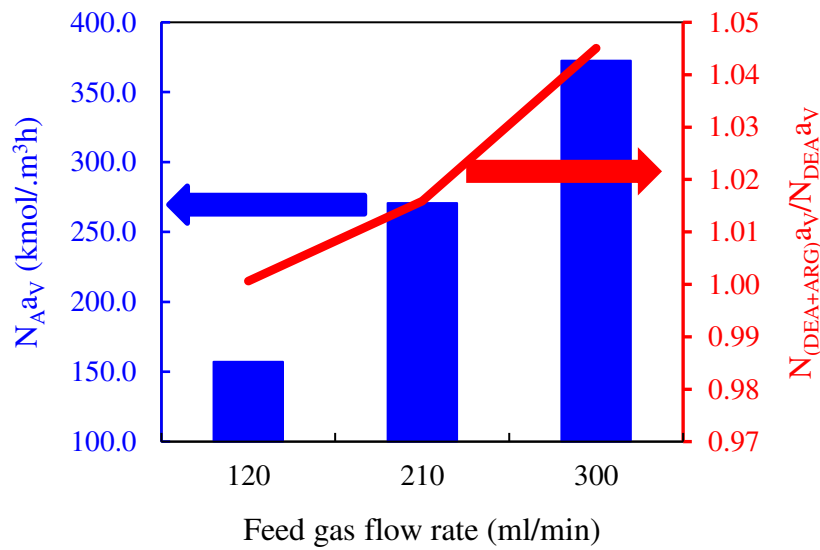287   costs by reducing the solvent circulation rate considering increased mass transfer flux.

Fig. 6. Effect of gas flow rate on volumetric molar flux and relative flux at 45 °C, Q_L =6.0

ml/min, and $C_{DEA\text{-}ARG}$ (23 12 wt%).

288

289   4.4. Response surface methodology

290   4.4.1. Analysis of variance

291   The results of ANOVA for both desired responses, namely K_Ga_v and θ, are shown in Table 3.

292   Concerning the concept of ANOVA statistical method, the significance of the factors and model

293   by RSM modeling is checked by the two parameters of p- and F-values, respectively. The

294   independent factors with higher p-values than 0.1 confirm a highly insignificant term, while lower

17

295 p-values than 0.001 exhibit their importance in the model (Behroozi et al. 2020). Based on the

296 results obtained from the models, all independent process variables significantly influence the final

297 θ and K_{Ga_V} values. Furthermore, high F-values of 636.14 and 1570.95 for the Θ and K_{Ga_v} models

298 imply their significance, as was consistent with the literature (Sarlak &Valeh-e-Sheyda 2022).

299 Additionally, among independent variables, the feed gas flow rate is the most significant

300 contributor to the CO_2 absorption in the mico-reactor due to its higher F-values than others.

301

302 Table 3. ANOVA results based on the RSM-FFD approach for Θ (%) and K_{Ga_V} (kmol.m^3.h.kPa)

303 in the CO_2 absorption process.

Source	CO$_2$ Absorption Efficiency (%)				Overall gas-phase mass transfer coefficient (kmol.m^3.h.kPa)				
	Sum of Squares	df	Mean Square	F-value	p-value Prob > F	Sum of Squares	df	Mean Square	F-value	p-value Prob > F
Model	270.76	7	38.68	660.80	< 0.0001	4453.00	7	636.14	1570.95	< 0.0001
A-Q_L	26.82	1	26.82	458.11	< 0.0001	166.13	1	166.13	410.26	< 0.0001
B-Q_G	217.15	1	217.15	3709.81	< 0.0001	4028.35	1	4028.35	9948.01	< 0.0001
C-C_{ARG}	6.56	1	6.56	112.14	< 0.0001	43.72	1	43.72	107.96	< 0.0001
AB	10.21	1	10.21	174.46	< 0.0001	59.85	1	59.85	147.80	< 0.0001
BC	1.83	1	1.83	31.18	< 0.0001	11.10	1	11.10	27.42	< 0.0001
A^2	1.97	1	1.97	33.62	< 0.0001	8.93	1	8.93	22.05	< 0.0001
B^2	4.36	1	4.36	74.53	< 0.0001	111.72	1	111.72	275.89	< 0.0001
Residual	1.40	24	0.059			9.72	24	0.40		
Lack of Fit	1.40	19	0.074		0.023	9.72	19	0.51		0.012
Pure Error	0.000	5	0.000			0.000	5	0.000		
Cor Total	272.16	31				4462.71	31			

304

305   Other results obtained from ANOVA are the statistical data for correlations prediction, as

306   presented in Table 4. In all cases, the standard deviation (*SD %*) of the models, as a measure of

307   dispersion, is quite low, implying that both models are highly reproducible. The coefficient of

308   variance (*C.V.%*) defines the ratio of the standard error to the average quantity of the detected

309   response as a percentage that exhibits the model reproducibility [39]. As a general rule of thumb,

310   a reasonably reproducible model has a coefficient variation (*C.V. %*) value lower than 10. The

311   values of *C.V. %* for Θ and $K_{G}a_v$ were reported as 0.26 and 1.19, suggesting the reliability and

312   precision of the experiments carried out. The determination coefficient (R^2) values have been

313   0.9948 and 0.9978 for Θ and $K_{G}a_v$, illustrating that the experimental data of both responses were

314   appropriately fitted.

315   Table 4. Statistical factors obtained from ANOVA for both predicted models of Θ and $K_{G}a_v$.

Factor	Θ	$K_{G}a_v$
Standard Deviation (*SD %*)	0.24	0.64
Mean	92.46	53.70
C.V.%	0.26	1.19
R^2	0.9948	0.9978
Adjusted-R^2	0.9933	0.9972
Predicted-R^2	0.9901	0.9959
Adequate Precision	89.379	122.928

316   The adequate precision demonstrates the signal-to-noise ratio computed by comparing the domain

317   of the estimated quantities at the design points to the mean estimation error. When the difference

318   between Adjusted-R^2 and Predicted-R^2 values is less than 0.2, rational compatibility between the

319   data is detected. The desirable model has an adequate ratio higher than 4, indicating acceptable

320   model discrimination (Behroozi et al. 2021). The proper signal for both models is achieved by the

321   adequate precision quantities, being 89.379 and 122.928 for the Θ and $K_{G}a_v$ responses,

322   respectively. Therefore, the achieved adopted models can be utilized for further analysis.

323   The histograms of residual distribution for CO_2 absorption efficiency and the overall gas-phase

324   mass transfer coefficient were plotted in Fig. 7. As exposed, the plot of externally studentized

325   residuals versus predicted response did not display any outliers, and all data are within -3.58606

326   and 3.58606. The dispersal of data in this range substantiated that neither the models violated the

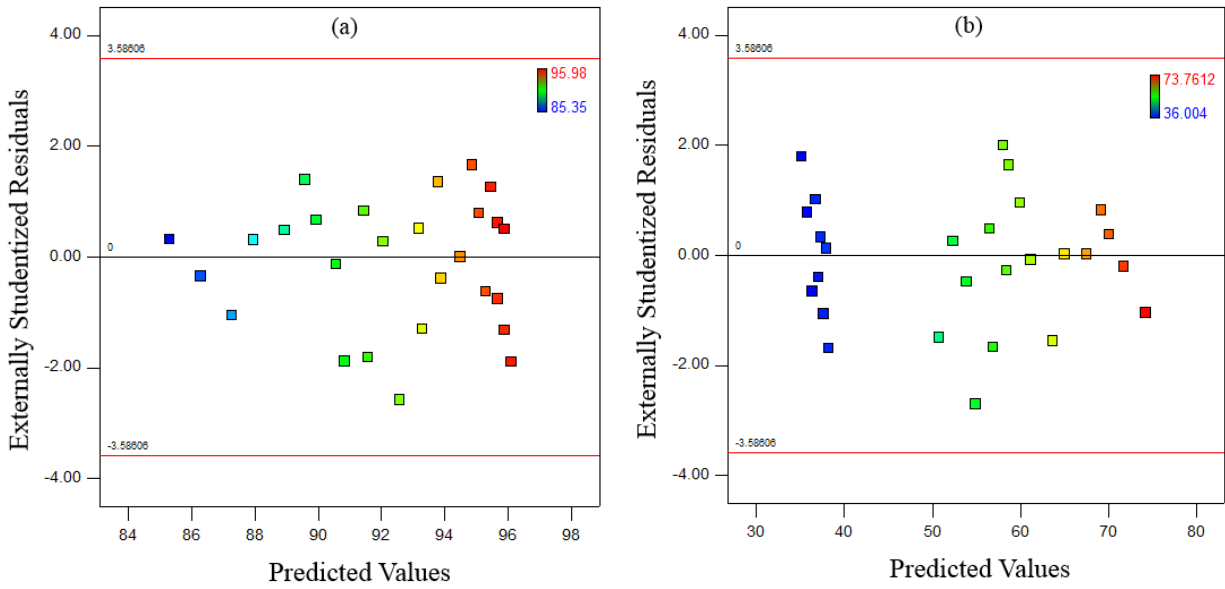327   independence nor the constant variance assumption.

Fig. 7. Studentized residual versus predicted values obtained from ANOVA for (a) Θ and (b) $K_G a_v$.

328

329   Based on the RSM-FFD modeling, the response functions are suggested in terms of actual factors

330   to predict both absorption efficiency and the overall gas-phase mass transfer coefficient, as given

331   in Eqs. (10) and (11), respectively. The positive signs before coefficients present the synergistic

332   effect of factor towards the response, whereas negative signs imply an antagonistic effect.

$$\theta(\%) = +97.530 + 0.375Q_L - 0.028Q_G + 0.076C_{ARG} + 3.416 \times 10^{-3} Q_L Q_G \qquad (10)$$
$$+1.083 \times 10^{-3} Q_G C_{ARG} - 0.057Q_L^2 - 9.461 \times 10^{-5} Q_G^2$$

$$K_G a_V \left(kmol\middle/ m^3.h.kPa\right) = +1.808 + 0.737Q_L + 0.296Q_G - 0.171C_{ARG} + 8.271 \times 10^{-3} Q_L Q_G \quad (11)$$
$$+ 2.672 \times 10^{-3} Q_G C_{ARG} - 0.121Q_L^2 - 4.787 \times 10^{-4} Q_G^2$$

333

334   4.4.2. Interaction effects

335   Three-dimensional (3D) surface plots for the measured responses, namely Θ and $K_G a_v$, were

336   displayed by Eqs. (10) and (11). In this case, two factors were assumed to be varied, while the

337   third factor was kept constant. Fig. 8a indicates that at a constant solvent concentration of DEA

338   ARG (27 8 wt%), and low feed gas flow rates of 120.0 ml/min, the CO_2 absorption efficiency

339   intensified as the inlet solvent flow rate increased from 3.0 to 6.0 ml/min and slightly decreased

340   as the absorbent flow rate increases from 6.0 to 90 ml/min. Finally, it is clear that in high gas flow

341   rate, Θ increases significantly with liquid flow rate, as the detention time of the solvent will be

342   short at the interface. Correspondingly the superficial renewal rate increases, resulting in the mass

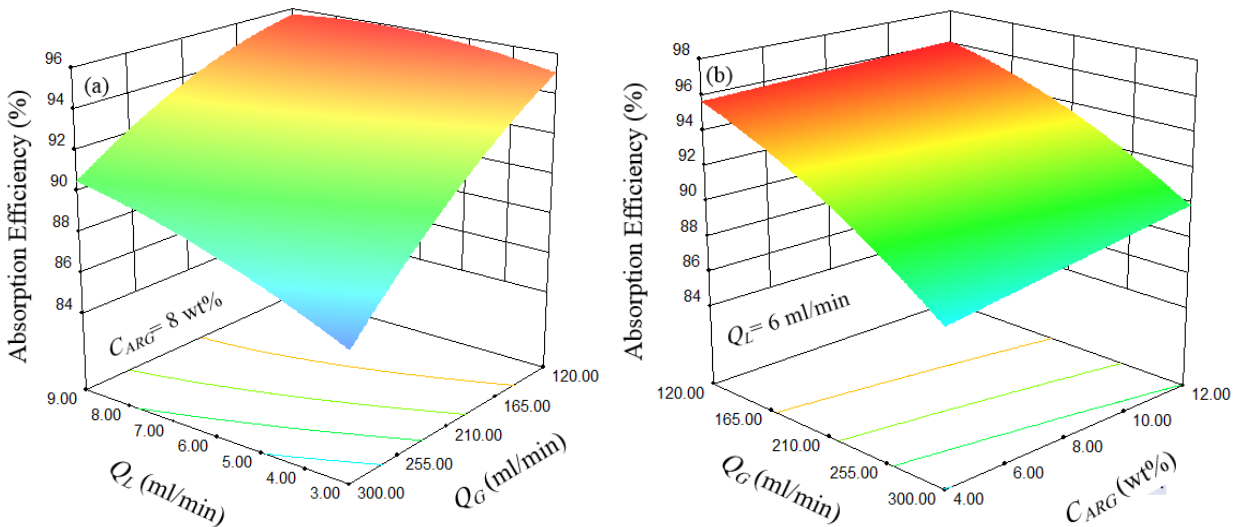343   transfer enhancement between the CO_2 and the solvent (Li et al. 2014).

Fig. 8. 3D response surfaces for Θ versus independent variables of (a) Q_L and Q_G, and (b) Q_G
and C_{ARG}; at 45°C, 1 atm, and $C_{DEA}=(35\text{-}C_{ARG})$ wt%.

344   Fig. 8b displays the interaction plot between the arginine concentration and the feed gas flow rate

345   for the aqueous mixture of DEA-ARG. The slight slope of the graph implies that though the impact

346   of amino acid concentration, C_{ARG}, is small on the absorption efficiency, as compared to the feed

347   gas flow but its effect is different at various ranges of the gas flow rates. Specifically, adding the

348   amino acid content from 4 to 12 wt% in ARG-DEA blended solution at high inlet gas flow rates

349   will positively influence the absorption efficiency, while increasing the amino acid concentration

350   at low gas flow rates of 120 ml/min negatively affects the absorption efficiency.

351   According to the 3D graph in Fig. 9, an increase in all variables has caused an improvement in the

352   volumetric gas-phase mass transfer coefficient. Comparing the graphs of Fig. 9a and b illustrates

353   that the influences of both variables of Q_L and Q_G on K_Ga_v increment are more tangible than the

354   effect of C_{ARG}; an increase in both flow rates from the minimum values to the maximum values

355   elevated K_Ga_V from 36.18 to 71.63 kmol/m^3.h.kPa. However, under low gas flow rates, an increase

356   in the presence of amino acid in the blended mixture of DEA: ARG improves the overall mass

357   transfer coefficient values by only 1.49%, while this value augments to more than 8.03 % under
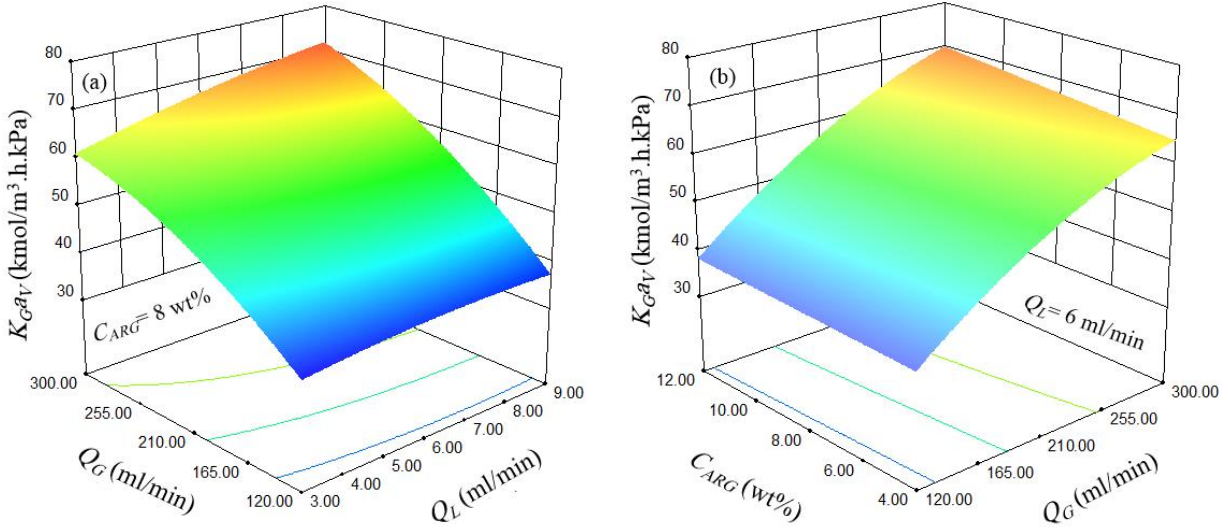
358   high flow rates of the feed gas.

359

Fig. 9. 3D response surfaces for K_Ga_v versus independent variables of (a) Q_L and Q_G, and (b) Q_G and C_{ARG}; at 45 °C, 1 atm, and $C_{DEA}=(35-C_{ARG})$ wt%.

360

361   4.4.3. Optimization framework by RSM modeling

362   The optimum experimental conditions for amine-amino acid-based CO_2 capture were investigated

363   by implementing RSM to determine the optimal parameters required to achieve high CO_2

364   absorption efficiency, $\Theta(\%)$, and overall gas-phase mass transfer coefficient, K_Ga_v (kmol/ m³. h.

365   kPa). Based on Table 5, from the optimization approach executed by the RSM model in Design-

366   Expert software, three independent process variables, including the feed gas flow rate, the inlet

367   DEA-ARG flow rate, and the concentration of the amino acid in the blended aqueous solution of

368   DEA-ARG were optimized within their studied ranges.

369

370

371

372   Table 5. The optimized numerical variables obtained for CO_2 absorption efficiency and overall

373   gas-phase mass transfer coefficient at 45 °C and 1 atm.

Name	Goal	Lower Limit	Upper Limit	Optimum value
A: Q_L (ml/min)	in range	3.0	9.0	9.0
B: Q_G (ml/min)	in range	120	300	263.40
C: C_{ARG} (wt%)	in range	4	12	12
θ (%)	maximize	85.35	95.98	92.93
K_Ga_v (kmol/m^3.h.kPa)	maximize	36.004	73.7612	69.40

374

375   The optimization process denotes that the concentration of ARG, as a promoting agent, highly

376   influences the efficiency of the CO_2 capture. Besides, it was noted that the CO_2 capture, predicted

377   by the model, achieved 92.93 % absorption efficiency with K_Ga_v of 69.40 kmol/m^3.h.kPa under

378   the Q_L of 9 ml/min, O_G of 263.4 ml/min, and solvent composition of DEA ARG (23 12 wt%).

379   Under the optimized input process variables, the experimental values for the θ and K_Ga_v were

380   92.27% and 68.96 kmol/m^3.h.kPa, corresponding to the deviation in predicted and observed values

381   of 0.71% and 0.63%, respectively.

382   Fig. 10 compares the range of K_Ga_v values for various gas-liquid contactors. As indicated, the

383   obtained ranges for K_Ga_v values in the designed micro-contactor are 2-3 orders of magnitude

384   higher, as compared with conventional absorption systems. This illustrates that the presence of

385   green arginine as a promoting agent not only intensifies the mass transfer coefficient but also, as a

386   green solvent alternative, intensifies the reactivity of the traditional aqueous solution of secondary
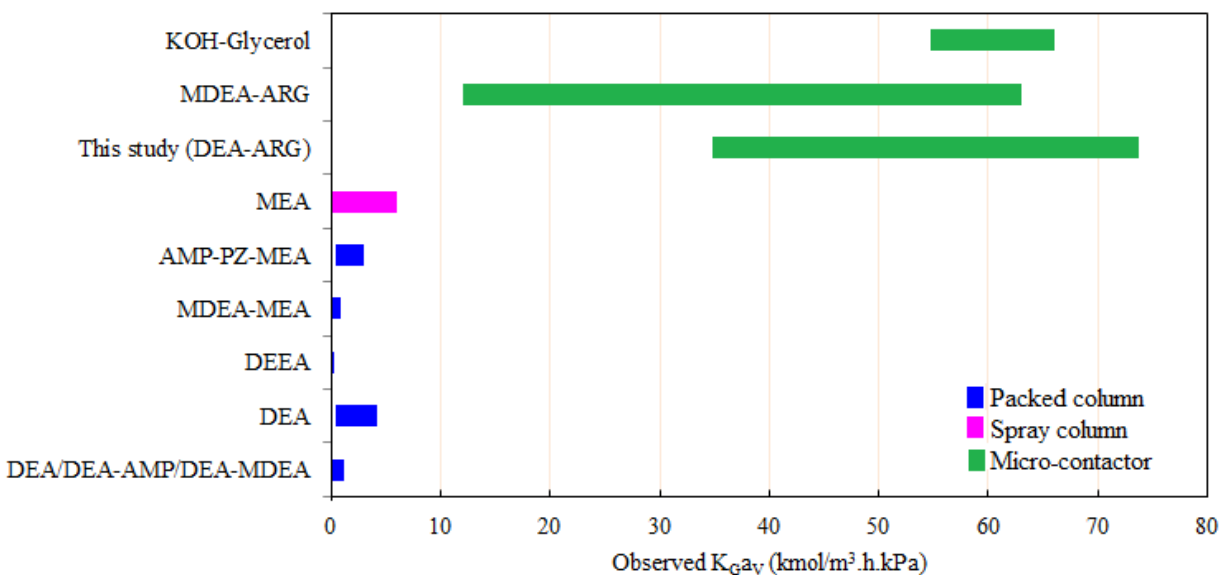
387   alkanolamines.

Fig. 10. Comparison of the overall mass transfer coefficients in various gas-liquid contactors (Aroonwilas &Veawab 2004, Kuntz &Aroonwilas 2009, Naami et al. 2013, Nakrak et al. 2021, Rashidi &Sahraei 2022, Sahraei et al. 2019, Sarlak &Valeh-e-Sheyda 2022, Xu et al. 2016).

388

389   5. Conclusion

390   In the current study, L-arginine amino acid was introduced as a promoting agent that highly

391   influence the carbon capture efficiency in an aqueous solution of secondary alkanolamine, DEA

392   35 wt%. The mass transfer characteristics of CO_2 was experimentally assessed into the blended

393   aqueous solution of DEA-ARG in terms of the CO_2 absorption efficiency, volumetric gas-phase

394   mass transfer coefficient, and mass flux in a T-type micro-contactor.

395   It was found that ARG, as a green acid-based promoter, could reduce the mass transfer resistance

396   in the liquid phase, particularly at high liquid flow rates, improving the mass transfer rate between

397   the gas and liquid phases. The empirical results revealed that the increase in contribution of ARG

398   intensifies the carbon capture in the blended solution of amine-amino-acid. Specifically, the mixed

25

399 DEA ARG (23 12 wt%) demonstrate the maximum absorption efficiency, volumetric gas-phase

400 mass transfer coefficient, and mass transfer flux.

401 For the blended aqueous solution of DEA ARG (23 12 wt%), an increase in the feed DEA-ARG

402 flow rate from 3.0 to 9.0 ml/min yielded an increment of 2.5% and 12.8% in the values of the Ө

403 (%) and $K_G a_V$. At a constant liquid flow rate of 6.0 ml/min, upon elevating the gas flow rate from

404 120.0 to 300.0 ml/min, the absorption efficiency was found to reduce by 5.95 %. However, the

405 values of K_{GaV} will augment from 37.40 to 62.98 kmol.m^3.h.kPa, corresponding to 68.39 %

406 intensification in the overall gas-phase mass transfer coefficient.

407 Furthermore, according to the optimization process by RSM modeling, the optimal working point

408 was proposed at 9.0 ml/min, 263.4 ml/min, DEA ARG (23 12 wt%), yielding the maximum values

409 of 92.93% efficiency and 69.40 kmol/m^3.h.kPa. In conclusion, the results highlight the potential

410 of the ARG, as a highly efficient promoter mixed with secondary alkanolamines, for practical

411 implementation in small-scale carbon capture applications in micro-contactor-based absorption

412 systems.

413

417

418 **Author Contributions**

419 *Peyvand Valeh-e-Sheyda* made substantial contributions to the Investigation, Methodology,

420 Resources, Formal analysis, Conceptualization, Review & Editing, Project administration, and

421 Supervision. The Investigation, Visualization, Data collection, Formal analysis, and Writing-

Original Draft of the manuscript was performed by *Forough Karimi. A*ll authors commented on previous versions of the manuscript. All authors read and approved the final manuscript.

References

Afkhamipour M, Mofarahi M (2017): Review on the mass transfer performance of CO2 absorption by amine-based solvents in low-and high-pressure absorption packed columns. RSC Advances 7, 17857-17872

Afkhamipour M, Mofarahi M (2018): Effects of operating parameters of packed columns on the KGav for CO2 absorption by amine solutions using optimization–simulation framework. Separation & Purification Technology 202, 86-102

Akkarawatkhoosith N, Nopcharoenkul W, Kaewchada A, Jaree A (2020): Mass Transfer Correlation and Optimization of Carbon Dioxide Capture in a Microchannel Contactor: A Case of CO2-Rich Gas. Energies 13, 5465

Aroonwilas A, Veawab A (2004): Characterization and comparison of the CO2 absorption performance into single and blended alkanolamines in a packed column. Industrial & engineering chemistry research 43, 2228-2237

Behroozi AH, Akbarzad N, Ghaemi A (2020): CO2 Reactive Absorption into an Aqueous Blended MDEA and TMS Solution: Experimental and Modeling. International Journal of Environmental Research 14

Behroozi AH, Saeidi M, Ghaemi A, Hemmati A, Akbarzad N (2021): Electrolyte solution of MDEA–PZ–TMS for CO2 absorption; response surface methodology and equilibrium modeling. Environmental Technology & Innovation 23, 101619

Caplow M (1968): Kinetics of carbamate formation and breakdown. Journal of the American Chemical Society 90, 6795-6803

Chowdhury FA, Goto K, Yamada H, Matsuzaki Y (2020): A screening study of alcohol solvents for alkanolamine-based CO2 capture. International Journal of Greenhouse Gas Control 99, 103081

Chu C, Zhang F, Zhu C, Fu T, Ma Y (2019): Mass transfer characteristics of CO2 absorption into 1-butyl-3-methylimidazolium tetrafluoroborate aqueous solution in microchannel. International Journal of Heat & Mass Transfer 128, 1064-1071

Chuah CY, Kim K, Lee J, Koh D-Y, Bae T-H (2019): CO2 absorption using membrane contactors: Recent progress and future perspective. Industrial & Engineering Chemistry Research 59, 6773-6794

Constantinou A, Gavriilidis A (2010): CO2 Absorption in a Microstructured Mesh Reactor. Industrial & Engineering Chemistry Research 49, 1041-1049

Danckwerts PV (1979): The reaction of CO2 with ethanolamines. Chemical Engineering Science 34, 443-446

Dang S, Qin B, Yang Y, Wang H, Cai J, Han Y, Li S, Gao P, Sun Y (2020): Rationally designed indium oxide catalysts for CO2 hydrogenation to methanol with high activity and selectivity. Science Advances 6, eaaz2060

Du Y, Wang Y, Rochelle GT (2017): Piperazine/4-hydroxy-1-methylpiperidine for CO2 capture. Chemical Engineering Journal 307, 258-263

Dutcher B, Fan M, Russell AG (2015): Amine-based CO2 capture technology development from the beginning of 2013☐ A Review. ACS Applied Materials & Interfaces 7, 2137-2148

Fashi F, Ghaemi A, Behroozi AH (2020): Piperazine impregnation on Zeolite 13X as a novel adsorbent for CO2 capture: experimental and modeling. Chemical Engineering Communications, 1-17

466 Ganapathy H, Steinmayer S, Shooshtari A, Dessiatoun S, Ohadi MM, Alshehhi M (2016): Process
467   intensification characteristics of a microreactor absorber for enhanced CO2 capture. Applied
468   Energy 162, 416-427

469 Ghaemi A, Behroozi AH (2020): Comparison of hydroxide-based adsorbents of Mg (OH) 2 and Ca (OH)
470   2 for CO2 capture: utilization of response surface methodology, kinetic, and isotherm modeling.
471   Greenhouse Gases: Science & Technology 10, 948-964

472 Haghtalab A, Gholami V (2019): Carbon dioxide solubility in the aqueous mixtures of diisopropanolamine+
473   l-arginine and diethanolamine+ l-arginine at high pressures. Journal of Molecular Liquids 288,
474   111064

475 Hasib-ur-Rahman M, Bouteldja H, Fongarland P, Siaj M, Larachi Fca (2012): Corrosion behavior of carbon
476   steel in alkanolamine/room-temperature ionic liquid based CO2 capture systems. Industrial &
477   Engineering Chemistry Research 51, 8711-8718

478 Hosseini-Ardali SM, Hazrati-Kalbibaki M, Fattahi M, Lezsovits F (2020): Multi-objective optimization of
479   post combustion CO2 capture using methyldiethanolamine (MDEA) and piperazine (PZ) bi-
480   solvent. Energy 211, 119035

481 Khuri AI, Mukhopadhyay S (2010): Response surface methodology. Wiley Interdisciplinary Reviews:
482   Computational Statistics 2, 128-149

483 Kittiampon N, Kaewchada A, Jaree A (2017): Carbon dioxide absorption using ammonia solution in a
484   microchannel. International Journal of Greenhouse Gas Control 63, 431-441

485 Kortunov PV, Siskin M, Baugh LS, Calabro DC (2015): In situ nuclear magnetic resonance mechanistic
486   studies of carbon dioxide reactions with liquid amines in non-aqueous systems: evidence for the
487   formation of carbamic acids and zwitterionic species. Energy & Fuels 29, 5940-5966

488 Kuntz J, Aroonwilas A (2009): Mass-transfer efficiency of a spray column for CO2 capture by MEA.
489   Energy Procedia 1, 205-209

490 Lam KF, Sorensen E, Gavriilidis A (2013): Review on gas–liquid separations in microchannel devices.
491   Chemical Engineering Research & Design 91, 1941-1953

492 Lei L, Lindbråthen A, Zhang X, Favvas EP, Sandru M, Hillestad M, He X (2020): Preparation of carbon
493   molecular sieve membranes with remarkable CO2/CH4 selectivity for high-pressure natural gas
494   sweetening. Journal of Membrane Science 614, 118529

495 Li C, Zhu C, Ma Y, Liu D, Gao X (2014): Experimental study on volumetric mass transfer coefficient of
496   CO2 absorption into MEA aqueous solution in a rectangular microchannel reactor. International
497   Journal of Heat and Mass Transfer 78, 1055-1059

498 Mahmud N, Benamor A, Nasser M, El-Naas MH, Tontiwachwuthikul P (2019): Reaction kinetics of carbon
499   dioxide in aqueous blends of N-methyldiethanolamine and L-arginine using the stopped-flow
500   technique. Processes 7, 81

501 Morken AK, Pedersen S, Nesse SO, Flø NE, Johnsen K, Feste JK, de Cazenove T, Faramarzi L, Vernstad
502   K (2019): CO2 capture with monoethanolamine: solvent management and environmental impacts
503   during long term operation at the Technology Centre Mongstad (TCM). International Journal of
504   Greenhouse Gas Control 82, 175-183

505 Muchan P, Saiwan C, Narku-Tetteh J, Idem R, Supap T, Tontiwachwuthikul P (2017): Screening tests of
506   aqueous alkanolamine solutions based on primary, secondary, and tertiary structure for blended
507   aqueous amine solution selection in post combustion CO2 capture. Chemical Engineering Science
508   170, 574-582

509 Naami A, Sema T, Edali M, Liang Z, Idem R, Tontiwachwuthikul P (2013): Analysis and predictive
510   correlation of mass transfer coefficient KGav of blended MDEA-MEA for use in post-combustion
511   CO2 capture. International Journal of Greenhouse Gas Control 19, 3-12

512 Nadeali A, Kalantari S, Yarmohammadi M, Omidkhah M, Ebadi Amooghin A, Zamani Pedram M (2020):
513   CO2 separation properties of a ternary mixed-matrix membrane using ultraselective synthesized
514   macrocyclic organic compounds. ACS Sustainable Chemistry & Engineering 8, 12775-12787

515 Nakrak S, Yurata T, Chalermsinsuwan B, Tontiwachwuthikul P, Sema T (2021): Preliminary mass transfer
516   performance of CO2 absorption into AMP-PZ-MEA ternary amines. Available at SSRN 3821405

Niu H, Pan L, Su H, Wang S (2009): Effects of design and operating parameters on CO2 absorption in microchannel contactors. Industrial & Engineering Chemistry Research 48, 8629-8634

Nwaoha C, Tontiwachwuthikul P, Benamor A (2018): CO2 capture from lime kiln using AMP-DA2MP amine solvent blend: A pilot plant study. Journal of Environmental Chemical Engineering 6, 7102-7110

Pashaei H, Ghaemi A, Behroozi AH, Mashhadimoslem H (2021): Hydrodynamic and mass transfer parameters for CO2 absorption into amine solutions and its blend with nano heavy metal oxides using a bubble column. Separation Science & Technology, 1-16

Rashidi H, Rasouli P, Azimi H (2022): A green vapor suppressing agent for aqueous ammonia carbon dioxide capture solvent: Microcontactor mass transfer study. Energy 244, 122711

Rashidi H, Sahraei M (2022): Investigation of carbon dioxide absorption process in a microreactor by potash-glycerol hybrid solvent. Journal of Separation Science and Engineering 13, 52-60

Rochelle GT (2012): Thermal degradation of amines for CO2 capture. Current Opinion in Chemical Engineering 1, 183-190

Sahraei S, Rashidi H, Valeh-e-Sheyda P (2019): Investigation of Operational parameters and Optimization of Flue Gas Carbon Dioxide Absorption Process by Diethanolamine via Response Surface Methodology. Journal of Separation Science and Engineering 11, 26-40

Sarlak S, Valeh-e-Sheyda P (2022): The contribution of l-Arginine to the mass transfer performance of CO2 absorption by an aqueous solution of methyl diethanolamine in a microreactor. Energy 239, 122349

Sreedhar I, Upadhyay U, Roy P, Thodur SM, Patel CM (2020): Carbon capture and utilization by graphenes-path covered and ahead. Journal of Cleaner Production, 124712

Su H, Wang S, Niu H, Pan L, Wang A, Hu Y (2010): Mass transfer characteristics of H2S absorption from gaseous mixture into methyldiethanolamine solution in a T-junction microchannel. Separation & Purification Technology 72, 326-334

Tarley CRT, Silveira G, dos Santos WNL, Matos GD, da Silva EGP, Bezerra MA, Miró M, Ferreira SLC (2009): Chemometric tools in electroanalytical chemistry: methods for optimization based on factorial design and response surface methodology. Microchemical Journal 92, 58-67

Wang R, Liu S, Wang L, Li Q, Zhang S, Chen B, Jiang L, Zhang Y (2019): Superior energy-saving splitter in monoethanolamine-based biphasic solvents for CO2 capture from coal-fired flue gas. Applied Energy 242, 302-310

Xu B, Gao H, Luo X, Liao H, Liang Z (2016): Mass transfer performance of CO2 absorption into aqueous DEEA in packed columns. International Journal of Greenhouse Gas Control 51, 11-17

Yang Z, Guo W, Mahurin SM, Wang S, Chen H, Cheng L, Jie K, Meyer III HM, Jiang D-e, Liu G (2020): Surpassing Robeson upper limit for CO2/N2 separation with fluorinated carbon molecular sieve membranes. Chem 6, 631-645

Yu X-Y (2016): Advances in Microfluidics: New Applications in Biology, Energy, and Materials Sciences. BoD–Books on Demand

Zahid U, Al Rowaili FN, Ayodeji MK, Ahmed UJIJoGGC (2017): Simulation and parametric analysis of CO2 capture from natural gas using diglycolamine. International Journal of Greenhouse Gas Control 57, 42-51

Zhang L-L, Wang J-X, Sun Q, Zeng X-F, Chen J-F (2012): Removal of nitric oxide in rotating packed bed by ferrous chelate solution. Chemical Engineering Journal 181-182, 624-629

Zhu C, Guo H, Chu C, Fu T, Ma Y (2020): Gas-liquid distribution and mass transfer of CO2 absorption into sodium glycinate aqueous solution in parallel multi-channel microreactor. International Journal of Heat & Mass Transfer 157, 119943

565